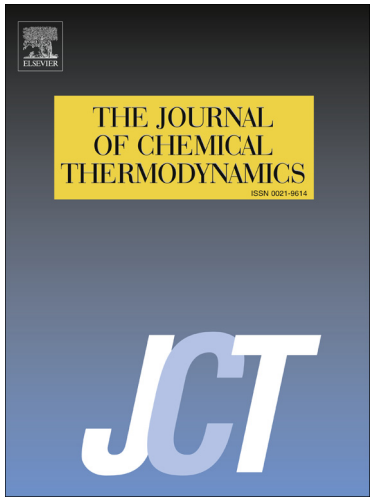

Coordination abilities of Good's buffer ionic liquids toward europium(III) ion in aqueous solution

Mohamed Taha, Imran Khan, João A.P. Coutinho

PII: S0021-9614(15)00400-0
DOI: http://dx.doi.org/10.1016/j.jct.2015.11.003
Reference: YJCHT 4451

To appear in: *J. Chem. Thermodynamics*

Received Date: 20 August 2015
Revised Date: 31 October 2015
Accepted Date: 2 November 2015

Please cite this article as: M. Taha, I. Khan, J.A.P. Coutinho, Coordination abilities of Good's buffer ionic liquids toward europium(III) ion in aqueous solution, *J. Chem. Thermodynamics* (2015), doi: http://dx.doi.org/10.1016/j.jct.2015.11.003

Coordination abilities of Good's buffer ionic liquids toward europium(III) ion in aqueous solution

*Mohamed Taha, Imran Khan, and João A. P. Coutinho**

CICECO-Aveiro Institute of Materials, Department of Chemistry, University of Aveiro, 3810-193 Aveiro, Portugal

Abstract

Good's buffer ionic liquids (GB-ILs) are new class of ILs with self-buffering capacity at the physiological pH range for biological research. GB-ILs are formed by the combination of Good's buffers as anions and various organic bases as counter ions. In this work, the complexation of europium(III) ion with tricine and tricine-based GB-ILs, tetramethylammonium tricinate, tetraethylammonium tricinate, tetrabutylammonium tricinate, cholinium tricinate, and 1-ethyl-3-methylimidazolium tricinate in aqueous solution were determined potentiometrically at 298.2 K and ionic strength I = 0.1 mol·dm^{-3} $NaNO_3$. The protonation constants of the studied ligands (L) and their overall stability constants ($\log\beta$) with Eu(III) were determined. The best model that fit the potentiometric data was consisted of six main species, EuL^{2+}, EuL_2^{+}, EuL_3, $EuH_{-1}L^{+}$, $EuH_{-2}L_2^{-}$, and $EuH_{-3}L_3^{3-}$. The $\log\beta_{Eu(tricine)}$, $\log\beta_{Eu(tricine)_2}$, and $\log\beta_{Eu(tricine)_3}$ are 5.75, 9.51, and 12.79, respectively. The overall stability constants ($\log\beta$) of tricine-based GB-ILs were found to be greater than those of tricine. The species distribution diagrams of these complexes were calculated and discussed in terms of percent Eu(III) and pH. We present a density functional theory (DFT) study to understand tricine chelating to Eu(III).

Keywords: Good's buffers ionic liquids; Eu(III) complexes; Tricine; Protonation constants; Stability constants.

---

*Corresponding author. Tel.: +351 234 401 507; Fax: + 351 234 370 084

E-mail address: jcoutinho@ua.pt (J. A. P. Coutinho)

1. Introduction

Ionic liquids (ILs) are a large class of salts with a low melting temperature below the boiling point of water at ambient pressure[1]. They usually consist entirely of ions, large organic cations (e.g., *N*-alkylimiazolium, *N*-alkylpyridinium, or tetraalkylamonium) and different inorganic (e.g., Cl^-, Br^-, I^-, $[BF_4]^-$ or $[PF_6]^-$) or organic (e.g., $[CF_3SO_3]^-$, $[CF_3CO_2]^-$, or $[N(SO_2CF_3)_2]^-$) anions with delocalized or shielded charges[1]. ILs are considered to be green alternatives to the volatile organic compounds (VOCs) volatile organic compounds (VOCs) because of their specific properties such as negligible vapor pressure, high chemical/thermal stability, high ionic conductivity, and high solvation ability for inorganic and organic compounds [1-4]. The most important feature of the ILs is their remarkable structural tenability, slight changes in the cationic and/or anionic groups have observed to produce different physicochemical properties, such as density, viscosity, polarity, and hydrophobicity; consequently, it is possible to designed ILs with some desired properties and classified as functionalized ILs or task-specific ILs (TSILs)[4]. The applications of ILs in all areas of chemical science are becoming increasingly popular in nearly the last 20 years, as reported in some recent reviews[1-4].

Application of ILs to substitute conventional solvents in liquid-liquid extraction of lanthanides and actinides has shown encourage results[5-9]. The IL-based extraction systems avoid many environmental problems related to the use of VOCs, which leads to safer processes. Another advantage of using ILs is that the metal ion can be recovered by electrodeposition [10]. However, the metal salts are poorly soluble in the traditional ILs. Several strategies to overcome this drawback have been attempted such as (1) the use of strong chelating agents, (2) the use of TSILs with chelating function groups on their cations and/or (3) the use of ILs with strong coordinating anions[11, 12].

The formation of stable complexes of europium (III) are of great interest due to their wide applications in optical devices and medical applications in magnetic resonance imaging, luminescence probes, and cancer treatment[13-17]. The affinity of some TSILs to Eu(III) has been also investigated and evaluated for Eu(III) extraction from aqueous solution [5].

Recently, we have synthesized novel ILs with buffer characteristics, in the physiological pH range, comprising anions derived from Good's buffers (e.g., tricine, TES, HEPES, MES, and CHES) and several cations such as 1-ethyl-3-methylimidazolium ($[C_2mim]^+$), tetramethylammonium ($[N_{1111}]^+$), tetraethylammonium ($[N_{2222}]^+$), tetrabutylammonium

($[N_{4444}]^+$), and cholinium ($[Ch]^+$) [18, 19]. Good's buffers were developed by Good *et al.* for use as biological buffers with high buffering capacity at the physiological pH range [20, 21]. Buffer capacity is a measure of a buffer's ability to resist change in pH with an added acid or base to the buffer solution. According to the Henderson–Hasselbalch equation, the buffering capacity of GB-ILs is maximum at the pH equal to the protonation constant of the amine group (pK_{a2}).

We are interested in determining the protonation constants tricine-based GB-ILs ([C_2mim][tricine], [N_{1111}][tricine], [N_{2222}][tricine], [N_{4444}][tricine], and [Ch][tricine]) and their complexation behavior with Eu(III). Tricine buffer is an interesting chelating agent due to its flexibility to behave as monodentate and multidentate ligand [22]. It is an *N*-substituted glycine and usually chelates with metal ions *via* carboxylate oxygen, amido nitrogen, and one or two hydroxymethyl groups. Tricine is capable of forming stable complexes with divalent alkaline-earth and transition metal ions, as well as lanthanides and actanides [22-31]. In this work, the stability constants of the complexes of tricine and tricine-based GB-ILs with Eu(III) ion in aqueous solution were determined by potentiometric technique. The geometries Eu(III)-tricine complexes were investigated by utilizing density functional theory with TZVP basis set.

2. Materials and Methods

2.1. Materials

Europium (III) nitrate pentahydrate, tricine, [C_2mim][OH], [N_{1111}][OH], [N_{2222}][OH], [N_{4444}][OH], [Ch][OH], sodium hydroxide, nitric acid, and potassium hydrogen phthalate, sodium nitrate, acetonitrile are analytical grade and obtained from commercial sources. The purity of these compounds were reported in Table 1. All materials were used as received without further purification. The synthesized tricine-based GB-ILs were purified by washing with acetone several times. Recrystallization of GB-ILs, except [C_2mim][tricine], from methanol-acetone mixture gave white powder, and dried by vacuum evaporation at room temperature. The purity levels of the synthesized tricine-based GB-ILs were determined by titration; a known mass of GB-IL was dissolved in pure water and titrated with standardized HCl, using the 'Metrohm 904' Titrando auto-titration apparatus (see section 2.3).

2.2. Synthesis of tricine-based Good's buffer ionic liquids

The tricine-based GB-ILs, [C_2mim][tricine], [N_{1111}][tricine], [N_{2222}][tricine], [N_{4444}][tricine], and [Ch][tricine], were synthesized by neutralizing a slight excess of equimolar tricine with the aqueous organic hydroxide aqueous solution as described in our earlier papers [18, 19]. The water content in the synthesized tricine-based GB-ILs was measured by Karl–Fischer coulometer using (Metrohm Ltd, model 831), and it was less than 0.05 wt %.

The molecular structures of the tricine-based GB-ILs were identified by ^{1}H and ^{13}C NMR spectroscopy (Bruker AMX 300) operating at 300.13 and 75.47 MHz, respectively. Chemical shifts are given in δ (ppm) relative to tetramethylsilane (TMS). The melting points of the tricine-based GB-ILs from the peak onset position were measured by differential scanning calorimetry (DSC), a Perkin Elmer DSC-7 instrument (Norwalk, CT), with heating rate of 5 °C min $^{-1}$ and N_2 flow of 40 mL·min^{-1}. The onset temperature was taken at the intersection of a line tangent where the DSC heat flow peak starts to develop, to the initial base-line. The DSC curves of [N_{1111}][tricine], [N_{2222}][tricine], [N_{4444}][tricine], and [Ch][tricine] are given in Fig. 1. It was observed that [N_{4444}][tricine] and [Ch][tricine] are hygroscopic compounds which absorb water during the DSC measurements; and thus, broad peaks are observed for these two compounds (Fig. 1). All the calculations considering tricine-based GB-ILs concentration were carried out discounting the complexed water.

[C_2mim][tricine]–^{1}H NMR (300 MHz, D_2O/TSP): 1.39 (*t,*3H), 3.86 (*s*, 3H), 4.20 (*q,* 2H), 7.65 (*s,*1H), 7.85 (*s*,1H), 9.58 (*s*,1H), 3.18 (*s*, 6H), 2.93 (*s*, 2H); ^{13}C NMR (300 MHz, D_2O/TSP): 15.29, 35.61, 44.10, 122.10, 123.66, 136.94, 60.41, 60.56, 177.10, 46.16.

[N_{1111}][tricine]–^{1}H NMR (300 MHz, D_2O/TSP): 3.11(*s,*12H), 3.19 (*s*, 6H), 2.87 (*s*, 2H); ^{13}C NMR (300 MHz, D_2O/TSP): 54.35, 60.55, 60.81, 176.10, 46.14.

[N_{2222}][tricine]– ^{1}H NMR (300 MHz, D_2O/TSP): 3.27(*q*, 8H), 1.26 (*m*, 12H), 3.52 (*s*, 6H), 3.30 (*s*, 2H); ^{13}C NMR (300 MHz, D_2O/TSP): 54.71, 9.39, 62.94, 63.14, 182.80, 47.69.

[N_{4444}][tricine]–^{1}H NMR (300 MHz, D_2O/TSP): 0.93 (*t,* 12H), 1.37 (*sext*, 8H), 1.65 (*quin*, 8H), 3.21 (*t*, 8H), 3.53 (*s*, 6H), 3.27 (*s*, 2H); ^{13}C NMR (300 MHz, D_2O/TSP): 15.71, 22.03, 26.00, 60.97, 62.93, 63.15, 182.83, 47.70.

[Ch][tricine]–^{1}H NMR (300 MHz, D_2O/TSP); δ *[Ch]*, 3.08 (*s*,9H), 3.38 (*m*, 2H), 3.93 (*m*, 2H), 3.42 (*s*, 6H), 3.17 (*s*, 2H); ^{13}C NMR (75.47 MHz, D_2O/TSP): 56.73, 58.47, 70.28, 63.30, 63.03, 182.19, 47.62.

2.3. Potentiometric measurements

In reporting the stability constants of the investigated complexes, the IUPAC guidelines for apparatus and measurements was followed [32-34]. The pH-potentiometric measurements were performed using the 'Metrohm 904' Titrando auto-titration unit equipped with a 801 magnetic stirrer, a Metrohm dosimat (model 683), a pH glass electrode (Metrohm 6.0262.100) with a precision of ± 0.001, Pt 1000/B/2 (Metrohm 6.1114.010), and titration vessel (a 70 cm^3 double-walled glass cell). This automatic titrator is connected to a laptop computer and the Tiamo 2.3 software was used to control the titration process. The titration vessel was equipped with a magnetic stirrer and a special lid with various inlets for holding the pH-electrode, burette tip, temperature probe, and a nitrogen gas inlet and outlet. This vessel was connected to a thermostatic water bath to maintain the solutions temperature. The purified water was degassed under vacuum at 70 ºC and cooled under nitrogen gas to be used in all the potentiometric measurements.

The glass pH electrode was calibrated in terms of proton concentration, p[H], by a strong acid-strong base titration with background electrolyte solution. The calibration mixture was consisted of 2 cm^{-3} of 0.1 $mol{\cdot}dm^{-3}$ HNO_3 and 50 cm^3 of 0.1 $mol{\cdot}dm^{-3}$ $NaNO_3$. This solution is titrated with 0.1 $mol{\cdot}dm^{-3}$ CO_2-free NaOH, was previously standardized against potassium hydrogen phthalate, in an N_2 atmosphere at (298.2 ± 0.1) K. The electrode potential (E, mV) values and NaOH increments (cm^3) were recorded and treated with GLEE software [35] to compute the standard electrode potential (E^o) and slope (s) of the Nernst equation, $E = E^\circ + s \log [H^+]$. The presence of carbonate in the calibration mixture was estimated using Gran plot, and was less than 1.0 %. The ion-product constant of water $pK_w = 13.78$ [36] was used as input to GLEE program.

2.4. The experimental runs

The reaction mixture used in the calculation of the protonation constants contained 1×10^{-3} $mol{\cdot}dm^{-3}$ ligand and 3×10^{-3} $mol{\cdot}dm^{-3}$ HNO_3. In order to calculate the stability constants of the binary complexes, the following solutions ware prepared: (a) 3×10^{-3} $mol{\cdot}dm^{-3}$ HNO_3 + 1×10^{-3} $mol{\cdot}dm^{-3}$ Eu(III) + 1×10^{-3} $mol{\cdot}dm^{-3}$ ligand, (b) 3×10^{-3} $mol{\cdot}dm^{-3}$ HNO_3 + 4×10^{-4} $mol{\cdot}dm^{-3}$ Eu(III) + 1×10^{-3} $mol{\cdot}dm^{-3}$ ligand, (c) 3×10^{-3} $mol{\cdot}dm^{-3}$ HNO_3 + 6×10^{-4} $mol{\cdot}dm^{-3}$ Eu(III) + 2×10^{-3} $mol{\cdot}dm^{-3}$ ligand, and (d) 3×10^{-3} $mol{\cdot}dm^{-3}$ HNO_3 + 1×10^{-3} $mol{\cdot}dm^{-3}$ Eu(III) + 4×10^{-4}

mol·dm^{-3} ligand; these solutions were conducted according to the Eu (III) to ligand ratios 1:1, 1:2.5, 1:3.3, and 2.5:1, respectively. The measurements were carried out at ionic strength I = 0.1 mol·dm^{-3} $NaNO_3$ and at 298.2 ± 0.1 K. The total volume of the titration solution was 50 cm^3, and 0.1 mol·dm^{-3} NaOH solution was added in 0.05 cm^3 increments to provide more than 150 experimental data points for each run. Each titration run was repeated three times. The nitrogen gas was bubbled through the solution for 5 min before starting the titration to remove the dissolved CO_2 and O_2., and the titration process was also proceed in nitrogen atmosphere.

2.5. Computation of protonation and stability constants.

The protonation and overall stability constants for tricine and GB-ILs were computed from the experimental pH-potentiometric measurements using the Hyperquad (Version 2008) [37]. The electrode potential (E, mV) data were converted to equivalent p[H] readings using the obtained E^o and slope s valued of the Nernst equation. The p[H] data and corresponding NaOH increments (cm^3) were used as input data for the Hyperquad program. The algorithm used in the Hyperquad program computes p[H] by solving a set of non-linear equations of mass-balance. The set of proposed complexes that show the best statistical fit and more chemical sensible was considered and included in this work. In the Hyperquad proram, the least-squares treatment was carried out by minimization of the sample standard deviation $\sigma = [\sum_i w_i (pH_i^{\mathrm{obs}} - pH_i^{\mathrm{calc}})^2 / (n-m)]^{1/2}$; where pH_i^{obs} and pH_i^{calc} are the observed and calculated pH values; n and m are the number of observations and number of parameters refined, respectively. The statistical weights $w_i = 1 / \sigma_i^2$, σ is the expected error of each experimental pH. For each system, the potentiometric data of the three different titration were treated together. The species distribution diagrams (SDD) of the investigated systems were computed with the Hyperquad Simulation and Speciation (HySS 2009) program [38].

2.6. Computational details

The geometries of Eu-tricine complexes were optimized in the conductor reference state (COSMO) by means of RI-DFT BP/COSMO method using the triple zeta valence plus polarization (TZVP) basis set with the TURBOMOLE 6.1 program [39]. The relativistic effective core potential (ECP) was applied for Eu atom[40].

3. Results and discussion

The structures of tricine and tricine-based GB-ILs are shown in Fig. 2. Representative titration profiles of tricine and $[N_{4444}]$[tricine], as well as their mixtures with Eu(III) are plotted in Fig. 3. The pH-potentiometric curves of the remaining systems are shown in Fig. 4 in the Supporting Information. The protonation constants of tricine and GB-ILs at I = 0.1 mol·dm^{-3} $NaNO_3$ and at 298.2 ± 0.1 K are reported in Table 2.

Tricine has two protonation sites attributed to the carboxylic group ($pK_{a1} = 2.68$) and the amino group ($pK_{a2} = 8.08$). The two pK_a values of tricine are in good agreement with the literature values [41]. From that table it is apparent that both pK_a values of tricine-based GB-ILs are lower than those of tricine. Fig. 5 shows the protonation equilibrium of $[N_{2222}]$[tricine], as an example. The decrease in the pK_a values of GB-ILs is probably due, at least in part, to the electrostatic interactions between the imidazolium, ammonium, or cholinium cations with the negatively charged carboxylic group of tricine anion (Fig 5), which stabilize the conjugate bases of GB-ILs, and thus facilitate the deprotonation process. The pK_a values follow the trend tricine > $[N_{1111}]$[tricine] > $[N_{2222}]$[tricine] ≅ $[N_{4444}]$[tricine] > $[C_2mim]$[tricine] ≅ [Ch][tricine].

From the potentiometric pH curves (Fig. 3 and Fig. 4) it is obvious that tricine and GB-ILs forms complexes with Eu(III) ion at least, because the buffer region of tricine is shifted to lower pH values. Best models to fit the potentiometric data of Eu(III) + tricine/GB-ILs mixtures reveal the formation of six complexes, including EuL^{2+}, EuL_2^+, EuL_3, $EuH_{-1}L^+$, $EuH_{-2}L_2^-$, and $EuH_{-3}L_3^{3-}$, as represented by Eq. (1):

$$p\mathrm{Eu} + q\mathrm{L} + r\mathrm{H} \rightleftharpoons \mathrm{Eu}_p\mathrm{L}_q\mathrm{H}_r, \qquad \beta_{pqr} = \frac{[\mathrm{Eu}_p\mathrm{L}_q\mathrm{H}_r]}{[\mathrm{Eu}]^p[\mathrm{L}]^q[\mathrm{H}]^r} \tag{1}$$

where L refers to tricine/ GB-ILs. The square-bracket symbol represents the species concentrations in mol·dm^{-3} unit. The symbols p, q, and r stand for the stoichiometric coefficients of Eu(III), L, and H^+ ions, respectively, where p = 1, q = 1, 2, or 3, r = -1, -2, or -3. It was necessary to involve the $EuH_{-1}L^+$, $EuH_{-2}L_2^-$, and $EuH_{-3}L_3^{3-}$ complexes in the proposed models to improve the goodness of fitting at higher pH. These species could be hydroxo-complexes or deprotonated complexes resulting from further deprotonation of a hydroxyl group of tricine. The calculated overall stability constants, $\log \beta_{pqr}$, of the Eu(III) complexes at 298.15 K and I = 0.1 mol·dm^{-3} $NaNO_3$ are summarized in Table 3. The stepwise stability constants

($\log K_{\mathrm{EuL}}$, $\log K_{\mathrm{EuL_2}}$, and $\log K_{\mathrm{EuL_3}}$) were calculated, aiming to evaluate the Eu(III) chelation capacity of tricine and tricine-based GB-ILs, which expressed by Eqs. (2-4).

$$Eu^{3+} + L^{-} \Leftrightarrow EuL^{2+}, \qquad \log K_{\mathrm{EuL}} = \frac{[EuL^{2+}]}{[Eu^{3+}][L^{-}]} \quad (2)$$

$$EuL^{2+} + L^{-} \Leftrightarrow EuL_2^{+}, \qquad \log K_{EuL_2} = \frac{[EuL_2^{+}]}{[EuL^{2+}][L^{-}]} \quad (3)$$

$$EuL_2^{+} + L^{-} \Leftrightarrow EuL_3, \qquad \log K_{EuL_3} = \frac{[EuL_3]}{[EuL_2^{+}][L^{-}]} \quad (4)$$

The values of the stepwise stability constants were reported in Table 4, where $\log K_{\mathrm{EuL}} = \log \beta_{110}$, $\log K_{\mathrm{EuL_2}} = \log \beta_{120} - \log \beta_{110}$, and $\log K_{\mathrm{EuL_3}} = \log \beta_{130} - \log \beta_{120}$.

It well known that glycine can act as a bidentate ligand with metal ions *via* the amino nitrogen and the carboxylate oxygen donors, and which is also capable of forming mono, bis and tris complexes forming stable five-membered chelate rings [42]. It is important to know whereas the hydroxyl oxygens of tricine, together with the amino nitrogen and the carboxylate oxygen, are involved in the coordination with Eu(III) ion. A first clue comes from comparing log*K* values of Eu(III) complexes with tricine and glycine. The fact that the corresponding log*K* values of Eu(glycine)$^{2+}$ and Eu(tricine)$^{2+}$ are 4.1 [43] and 5.75, respectively. This is a clear indication that at least one hydroxyl group of tricine is participated. If the stability of Eu(tricine)$^{2+}$ complex was only governed by the basicity of the amino group, its stability would be considerably below the stability of the Eu(glycine)$^{2+}$ complex because the basicity of tricine ($\mathrm{p}K_{a2}$ = 8.08) is about one and half pH unit smaller than that of glycine ($\mathrm{p}K_{a2}$ = 9.69, at 298.15 K and I = 0.1 mol·dm^{-3} KNO_3[44]). The same conclusion was observed by Fisher *et al*. for metal ion/Tris, 2-amino-2(hydroxymethyl)-1,3-propanediol($(HOCH_2)_3CNH_2$)), complexes. The tris(hydroxymethyl) methylamino part of tricine is comparable with the structure of Tris, and for this reason tricine is derived from the names tris and glycine. Moreover, it is clear from Table 4 that $\log K_{\mathrm{EuL}}$ values of tricine-based GB-ILs are greater than that of tricine. The reverse was also expected because the basicity of the amino group ($\mathrm{p}K_{a2}$) of GB-ILs was lower than that of tricine, indicating that the Eu(III)/tricine-hydroxo bonds are enhanced in presence of the studied cations. There are available crystal structures of tricine with some metal ions in which tricine acts as tridentate ligand and forms two five-membered ring, binding through the nitrogen atom of

the amino group and the oxygen atom of the carboxyl and side hydroxyl groups [24, 45-48]. These studies comprise monomeric complexes such as ML_2 (M = Cu (II), Ni(II), Zn(II))[45, 46] and a one dimensional Cu (II) chain. In both complexes, monomeric and 1D Cu(II) chain, the carboxylate group of tricine is in a deprotonated form[24]. A deprotonation of a hydroxyl group was observed in the formation of an alkoxo-bridged dimethyltin(IV) complex of tricine[47], while deprotonation of two hydroxyl groups result in an enneanuclear Fe(III) complex with tricine and 2-phenoxybenzoate [48]. Therefore, the obtained $EuH_{-1}(tricine)^{+}$, $EuH_{-2}(tricine)_2^{-}$, and $EuH_{-3}(tricine)_3^{3-}$ complexes could be due to the deprotonated of CH_2OH tricine arm. The $Eu(tricine)^{2+}$and the deprotonated $EuH_{-1}(tricine)^{+}$ complexes were optimized by RI-DFT-BP/COSMO method using TZVP basis set and a relativistic ECP on the Eu(III) atom, and their optimized structures are shown in Fig. 6. It is was found that tricine behaves as tetradentate ligand in both complexes. Nevertheless, in case of bis and tris complexes the tricine-hydroxo bonds appear to be broken because the values of the $\log K_{EuL_2}$ and $\log K_{EuL_3}$ are lower than those of $\log K_{EuL}$, in which the stepwise stability constants follow the order $\log K_{EuL} > \log K_{EuL_2} > \log K_{EuL_3}$.

The species distribution diagrams (SDD) were generated for [L]:[Eu(III)] ratio 3:1 using the proposed models and the Eu(III) hydrolysis constants, $Eu(OH)_n^{3-n}$ (n = 0–4) [49]. The reported $\log\beta$ for $Eu(OH)^{2+}$, $Eu(OH)_2^{+}$, $Eu(OH)_3$, and $Eu(OH)_4^{-}$ at (I = 0; T = 298.15 K) are -7.64, -15.1, -23.7, and -36.2, respectively [49]. The SDD of Eu–tricine and Eu–GB-IL models are given in Fig. 4. From the analysis of SDD it is clear that $Eu(tricine)^{2+}$, $Eu(tricine)_2^{+}$, and $Eu(tricine)_3$ complexes predominate at ~pH 6.2, 8.0, and 8.5, with concentrations exceed 80 %, 40 %, and 20 % the total Eu(III), respectively (Fig. 7). The concentrations of $Eu(GB\text{-}ILs)^{2+}$ and $Eu(GB\text{-}ILs)_3$ are similar to the $Eu(tricine)^{2+}$ and $Eu(tricine)_3$, respectively. While the concentrations of $Eu(GB\text{-}ILs)_2^{+}$ are greater than that of $Eu(tricine)_2^{+}$. The formation of EuL^{2+}, EuL_2^{+}, and EuL_3 was able to suppress the formation of the $Eu(OH)^{+2}$ and $Eu(OH)_2^{+}$ species below pH 10. The $Eu(OH)_3$ started to form with a maximum concentration *ca.* 80 % at pH 11, and $Eu(OH)_4^{-}$ species are formed above pH 11. The $EuH_{-1}(tricine)^{+}$, $EuH_{-2}(tricine)_2^{-}$, and $EuH_{-3}(tricine)_3^{3-}$ species are formed at pH 8.9, 9.4, and 11.2, with concentration reached *ca.* 14 %, 29 %, and 11 %, respectively. The concentrations of $EuH_{-1}(GB\text{-}ILs)^{+}$ do not significantly different from that of$EuH_{-1}(tricine)^{+}$, whereas the concentrations of $EuH_{-2}(GB\text{-}ILs)_2^{-}$ were

higher than that of $EuH_{-2}(tricine)_2^-$. The SDD clearly show that $EuH_{-3}([tetraalkylammonium][tricine])_3^{3-}$ are formed with minor concentrations. The formation of $EuH_{-3}([Ch][tricine])_3^{3-}$ and $EuH_{-3}([C_2mim][tricine])_3^{3-}$ were greater than that of $EuH_{-3}(tricine)_3^{3-}$.

4. Conclusion

In this work, the formation of complex species of europium (III) with tricine and tricine-based Good's buffer ionic liquids (GB-ILs = $[N_{1111}][tricine]$, $[N_{2222}][tricine]$, $[N_{4444}][tricine]$, [Ch][tricine], and $[C_2mim][tricine]$), was evaluated using potentiometric technique, at fixed total–ligand and total–metal concentration ratio, at 298.2 ± 0.1 K and 0.1 mol·dm^{-3} $NaNO_3$ ionic strength. The pK_a values of tricine and tricine-based GB-ILs were first calculated. The pK_a values of tricine-based GB-ILs were found be lower than that of tricine. The overall stability constants, $\log \beta$, of the Eu(III)-tricine/GB-ILs complexes were calculate from the potentiometric data. Six main species, EuL^{2+}, EuL_2^+, EuL_3, $EuH_{-1}L^+$, $EuH_{-2}L_2^-$, and $EuH_{-3}L_3^{3-}$, were identified for all systems studied, and the $\log \beta$ values were greater for Eu(III)–GB-ILs complexes than those of Eu(III)-tricine complexes. The results reveal that at least one hydroxyl group of tricine (*N*-substituted glycine) involves in the coordination, in addition to amino nitrogen and the carboxylate oxygen donors. Moreover, DFT study on $Eu(tricine)^{2+}$ and the deprotonated $EuH_{-1}(tricine)^+$ complexes shows that tricine acts as tetradentate ligand. The species distribution diagrams for all systems were computed and discussed.

Acknowledgment

This work was financed by national funding from Fundação para a Ciência e a Tecnologia (FCT, Portugal), European Union, QREN, FEDER and COMPETE for funding the CICECO (project PEst-C/CTM/LA0011/2013), QOPNA (project PEst-C/QUI/UI0062/2013) and LSRE/LCM (project PEst-C/EQB/LA0020/2013). M. Taha and I. Khan acknowledge FCT for the postdoctoral grants SFRH/BPD/78441/2011 and SFRH/BPD/76850/2011, respectively.

References

[1] N.V. Plechkova, K.R. Seddon, Chem. Soc. Rev. 37 (2008) 123-150.
[2] T. Welton, Chem. Rev. 99 (1999) 2071-2084.
[3] M.G. Freire, A.F.M. Claudio, J.M. Araujo, J.A. Coutinho, I.M. Marrucho, J.N.C. Lopes, L.P.N. Rebelo, Chem. Soc. Rev. 41 (2012) 4966-4995.
[4] N.V. Plechkova, K.R. Seddon, Ionic liquids:"designer" solvents for green chemistry, Methods and Reagents for Green Chemistry, (2007) 105-130.
[5] A. Rout, K. Binnemans, Dalton Trans. 43 (2014) 1862-1872.
[6] A. Rout, K. Binnemans, Dalton Trans. 43 (2014) 3186-3195.
[7] X. Sun, H. Luo, S. Dai, Dalton Trans. 42 (2013) 8270-8275.
[8] X. Huang, Q. Zhang, J. Liu, H. He, W. Zhu, X. Wang, J. Radioanal. Nucl. Ch. 298 (2013) 41-46.
[9] P.K. Mohapatra, A. Sengupta, M. Iqbal, J. Huskens, S.V. Godbole, W. Verboom, Dalton Trans. 42 (2013) 8558-8562.
[10] S.C. Hsu, C.-J. Su, F.-L. Yu, W.-J. Chen, D.-X. Zhuang, M.-J. Deng, I.-W. Sun, P.-Y. Chen, Electrochim. Acta 54 (2009) 1744-1751.
[11] M.V. Mancini, N. Spreti, P. Di Profio, R. Germani, Sep. Purif. Technol. 116 (2013) 294-299.
[12] A. Messadi, A. Mohamadou, S. Boudesocque, L. Dupont, E. Guillon, Sep. Purif. Technol. 107 (2013) 172-178.
[13] V. Trusova, A. Yudintsev, L. Limanskaya, G. Gorbenko, T. Deligeorgiev, J. Fluoresc. 23 (2013) 193-202.
[14] I. Boldyrev, G. Gaenko, E. Moiseeva, T. Deligeorgiev, S. Kaloyanova, N. Lesev, A. Vasilev, J. Molotkovsky, Russ. J. Bioorganic Chem. 37 (2011) 364-368.
[15] G. Momekov, T. Deligeorgiev, A. Vasilev, K. Peneva, S. Konstantinov, M. Karaivanova, Med. Chem. 2 (2006) 439-445.
[16] P. Escribano, B. Julián-López, J. Planelles-Aragó, E. Cordoncillo, B. Viana, C. Sanchez, J. Mater. Chem. 18 (2008) 23-40.
[17] R. Singh, H.S. Nalwa, J. Biomed. Nanotechnol. 7 (2011) 489-503.
[18] M. Taha, F. e Silva, M.V. Quental, S.P.M. Ventura, M.G. Freire, J.A.P. Coutinho, Green Chem., (2014) 3149–3159.
[19] M. Taha, M.R. Almeida, F.A.e. Silva, P. Domingues, S.P.M. Ventura, J.A.P. Coutinho, M.G. Freire, Chem. Eur. J. 21 (2015) 4781-4788.
[20] N.E. Good, G.D. Winget, W. Winter, T.N. Connolly, S. Izawa, R.M. Singh, Biochemistry, 5 (1966) 467-477.
[21] W.J. Ferguson, K. Braunschweiger, W. Braunschweiger, J.R. Smith, J.J. McCormick, C.C. Wasmann, N.P. Jarvis, D.H. Bell, N.E. Good, Anal. Biochem. 104 (1980) 300-310.
[22] R.C. Kapoor, J.K. Jailwal, J. Kishan, J. Inorg. Nucl. Chem. 40 (1978) 155-158.
[23] M.M.A. Mohamed, Ann Chim(Rome) 97 (2007) 759-770.
[24] M. Ramos Silva, J.A. Paixao, A. Matos Beja, L. Alte da Veiga, Acta Crystallogr., Sect. C 57 (2001) 9-11.
[25] A.A.A. Boraei, I.T. Ahmed, Synth. React. Inorg. Met.-Org. Chem. 32 (2002) 981-1000.
[26] M.M. Khalil, A.M. Radalla, A.G. Mohamed, J. Chem. Eng. Data 54 (2009) 3261-3272.
[27] I.T. Ahmed, J. Chem. Eng. Data 48 (2003) 272-276.
[28] O.M. El-Roudi, S.A. Abdel-Latif, J. Chem. Eng. Data 49 (2004) 1193-1196.
[29] O.M. El-Roudi, E.M. Abd Alla, S.A. Ibrahim, J. Chem. Eng. Data 42 (1997) 609-613.
[30] M.E. Zayed, R.A. Ammar, J. Saudi Chem. Soc. 18 (2014) 774-782.
[31] M.M. Khalil, M. Taha, Monatsh. Chem/Chem. Mon. 135 (2004) 385-395.
[32] O. Yamauchi, A. Odani, Pure Appl. Chem. (1996) 469.
[33] A. Braibanti, G. Ostacoli, P. Paoletti, L.D. Pettit, S. Sammartano, Pure Appl. Chem. (1987) 1721.
[34] S. Sjöberg, Pure Appl. Chem. (1997) 1549.

[35] P. Gans, B. O'Sullivan, Talanta 51 (2000) 33-37.
[36] R.F. Jameson, M.F. Wilson, J. Chem. Soc., Dalton Trans., (1972) 2607-2610.
[37] P. Gans, A. Sabatini, A. Vacca, Talanta, 43 (1996) 1739-1753.
[38] L. Alderighi, P. Gans, A. Ienco, D. Peters, A. Sabatini, A. Vacca, Coord. Chem. Rev. 184 (1999) 311-318.
[39] A. Schafer, A. Klamt, D. Sattel, J.C.W. Lohrenz, F. Eckert, Phys. Chem. Chem. Phys. 2 (2000) 2187-2193.
[40] M. Dolg, H. Stoll, A. Savin, H. Preuss, Theoret. Chim. Acta 75 (1989) 173-194.
[41] R.N. Goldberg, N. Kishore, R.M. Lennen, J. Phys. Chem. Ref. Data 31 (2002) 231-370.
[42] T. Kiss, I. Sovago, A. Gergely, Pure Appl. Chem. 63 (1991) 597-638.
[43] S.P. Tanner, G.R. Choppin, Inorg. Chem. 7 (1968) 2046-2048.
[44] R.M. Keefer, J. Am. Chem. Soc. 68 (1946) 2329-2331.
[45] E.-J. Gao, L.-N. Ding, M.-S. Chen, Y.-G. Sun, L.-L. He, Acta Crystallogr., Sect. E 61 (2005) m2720-m2721.
[46] L. Menabue, M. Saladini, J Crystallogr Spectrosc Res. 22 (1992) 713-719.
[47] X.-N. Fang, Q.-Y. Luo, X.-R. Zeng, Y. Sui, X.-F. Li, Acta Crystallogr., Sect. E 61 (2005) m2604-m2606.
[48] K. Graham, A. Ferguson, F.J. Douglas, L.H. Thomas, M. Murrie, Dalton Trans. 40 (2011) 3125-3127.
[49] M.H. Bradbury, B. Baeyens, Geochim. Cosmochim. Ac. 66 (2002) 2325-2334.

Table 1 The specification of chemical samples.

Chemicals	Source	Purification method	Mass fraction purity	Melting point (*K*)
Europium (III) nitrate pentahydrate	Sigma-Aldrich	none	> 0.999[a]	—
Tricine	Sigma-Aldrich	none	> 0.990[a]	—
$[C_2mim][OH]$ (10 wt % in H_2O)	Sigma-Aldrich	none	—	—
$[N_{1111}][OH]$ (25 wt % in H_2O)	Sigma-Aldrich	none	—	—
$[N_{2222}][OH]$ (25 wt % in H_2O)	Sigma-Aldrich	none	—	—
$[N_{4444}][OH]$ (40 wt % in H_2O)	Sigma-Aldrich	none	—	—
[Ch][OH] (46 wt % in methanol)	Sigma-Aldrich	none	—	—
$[C_2mim]$[tricine]	Present work	none	0.983	viscous liquid
$[N_{1111}]$[tricine]	Present work	recrystallization and vacuum evaporation	0.990	388.9
$[N_{2222}]$[tricine]	Present work	recrystallization and vacuum evaporation	0.989	441.8
$[N_{4444}]$[tricine]	Present work	recrystallization and vacuum evaporation	0.985	370.8
[Ch][tricine]	Present work	recrystallization and vacuum evaporation	0.990	336.8
Sodium hydroxide	Eka Chemicals	none	—	—
Nitric acid (65 wt%)	Panreac (Barcelona, Spain)	none	—	—
Potassium hydrogen phthalate	Panreac (Barcelona, Spain)	none	> 0.998[a]	—
Sodium nitrate	Himedia Labs	none	> 0.995[a]	—
Methanol		none	> 0.999[a]	—
Acetonitrile	Lab-Scan (Ireland)	none	> 0.997[a]	—
Acetone	VWR Chemicals	none	> 0.995	—

Mass fraction purity determined by:
[a] The manufacturer
[b] Titration
Standard uncertainty of the melting point is $u(T) = 0.1$ K

Table 2. Protonation constants of tricine/ILs in water at 298.2 K, I = 0.1 mol·dm^{-3} ionic strength, and at 101.3 kPa[a].

tricine/tricine-ILs	pKa_1	standard deviation	pKa_2	standard deviation
tricine	2.68	0.03	8.08	0.02
$[N_{1111}]$[tricine]	2.66	0.05	8.02	0.01
$[N_{2222}]$[tricine]	2.65	0.05	7.95	0.02
$[N_{4444}]$[tricine]	2.65	0.04	7.96	0.007
[Ch][tricine]	2.60	0.02	7.87	0.008
$[C_2mim]$[tricine]	2.64	0.02	7.90	0.02

[a] standard uncertainty is $u(T)$ = 0.1 K; $u(P)$ = ± 1 kPa.

Table 3. The overall stability constants (log β_{pqr}) for Eu(III) complexes with tricine/ILs at 298.2 K, I = 0.1 mol·dm^{-3} ionic strength, and at 101.3 kPa[a].

species	(p,q,r)	Logβ_{pqr}	standard deviation	species	(p,q,r)	Logβ_{pqr}	standard deviation
tricine				[N_{1111}][tricine]			
	(1,1,0)	5.75	0.03		(1,1,0)	6.02	0.02
	(1,1,-1)	-2.80	0.09		(1,1,-1)	-2.54	0.08
	(1,2,0)	9.51	0.06		(1,2,0)	10.01	0.03
	(1,2,-2)	-8.30	0.05		(1,2,-2)	-7.93	0.03
	(1,3,0)	12.79	0.07		(1,3,0)	13.26	0.07
	(1,3,-3)	-15.45	0.07		(1,3,-3)	-17.04	0.20
[N_{2222}][tricine]				[N_{44444}][tricine]			
	(1,1,0)	5.90	0.02		(1,1,0)	6.01	0.02
	(1,1,-1)	-2.82	0.10		(1,1,-1)	-2.57	0.09
	(1,2,0)	9.77	0.05		(1,2,0)	10.01	0.03
	(1,2,-2)	-8.16	0.04		(1,2,-2)	-7.82	0.04
	(1,3,0)	12.84	0.14		(1,3,0)	13.12	0.08
	(1,3,-3)	-16.91	0.19		(1,3,-3)	-15.87	0.09
[Ch][tricine]				[C_2mim][tricine]			
	(1,1,0)	6.04	0.02		(1,1,0)	6.06	0.01
	(1,1,-1)	-2.61	0.10		(1,1,-1)	-2.33	0.05
	(1,2,0)	10.08	0.04		(1,2,0)	10.26	0.02
	(1,2,-2)	-7.54	0.04		(1,2,-2)	-7.45	0.02
	(1,3,0)	13.27	0.09		(1,3,0)	13.30	0.14
	(1,3,-3)	-14.65	0.04		(1,3,-3)	-14.46	0.06

[a] standard uncertainty is $u(T)$ = 0.1 K; $u(P)$ = ± 1 kPa.

Table 4. The stepwise stability constants for Eu(III) Complexes with tricine/ILs at 298.2 K, I = 0.1 mol·dm^{-3} ionic strength, and at 101.3 kPa[a].

species	$\log K_{EuL}$	$\log K_{EuL_2}$	$\log K_{EuL_3}$
tricine	5.75	3.76	3.28
$[N_{1111}]$[tricine]	6.02	3.99	3.25
$[N_{2222}]$[tricine]	5.90	3.87	3.07
$[N_{4444}]$[tricine]	6.01	4.00	3.11
[Ch][tricine]	6.04	4.04	3.19
$[C_2mim]$[tricine]	6.06	4.20	3.04

[a] standard uncertainty is $u(T)$ = 0.1 K; $u(P)$ = ± 1 kPa.

Figure Captions

Fig. 1. DSC melting curves of (a) [Ch][tricine], (b) [N_{4444}][tricine], [N_{2222}][tricine], and [N_{1111}][tricine].

Fig. 2. Chemical structures of tricine and tricine-based Good's buffer ionic liquids.

Fig. 3. pH titration curves of Eu(III) with tricine and [N_{4444}][tricine] at [T_L] = $1 \cdot 10^{-3}$ mol·dm^{-3} and [T_{Eu}] = $4 \cdot 10^{-4}$ mol·dm^{-3}, and at 298.2 K, I = 0.1 mol·dm^{-3} $NaNO_3$, and at 101.3 kPa. The symbols: (■) tricine; (▲) tricine + Eu(III); (□) [N_{4444}][tricine]; and (●)[N_{4444}][tricine] + Eu(III). The solid and dashed lines are the calculated pH from the refinement operations.

Fig. 4. pH titration curves of Eu(III) with (a) [C_4mim][tricine], (b) [Ch][tricine], (c) [N_{1111}][tricine], and (d) [N_{2222}][tricine] at [T_L] = $1 \cdot 10^{-3}$ mol·dm^{-3} and [T_{Eu}] = $4 \cdot 10^{-4}$ mol·dm^{-3}, and at 298.2 K, I = 0.1 mol·dm^{-3} $NaNO_3$, and at 101.3 kPa. The symbols: (■) tricine/IL and (▲) tricine/ILs + Eu(III). The solid and dashed lines are the calculated pH from the refinement operations.

Fig. 5. The protonation equilibrium of [N_{2222}][tricine].

Fig. 6. The optimized structures of $Eu(tricine)^{2+}$ and $EuH_{-1}(tricine)^{+}$complexes with DFT/TZVP levels. The atom distances are in angstroms.

Fig. 7. Species-distribution diagrams of Eu(III) with (a) tricine, (b) [N_{1111}][tricine], (c) [N_{2222}][tricine], (d) [N_{4444}][tricine], (e) [Ch][tricine], and (f) [C_2mim][tricine]; [Eu] =$4.0 \cdot 10^{-4}$ mol·dm^{-3} and [L] = $1.2 \cdot 10^{-3}$ mol·dm^{-3}; at 298.2 K, I = 0.1 mol·dm^{-3} $NaNO_3$, and at 101.3 kPa.

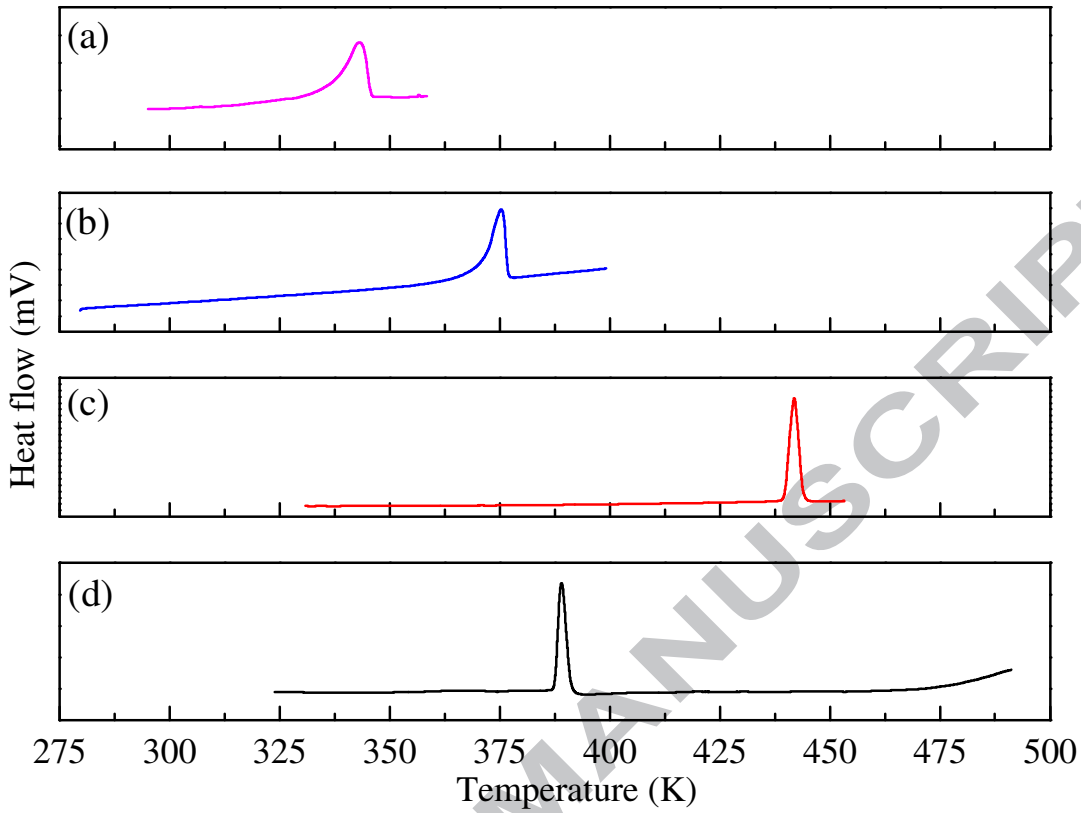

Fig. 1. DSC melting curves of (a) [Ch][tricine], (b) [N_{4444}][tricine], [N_{2222}][tricine], and [N_{1111}][tricine].

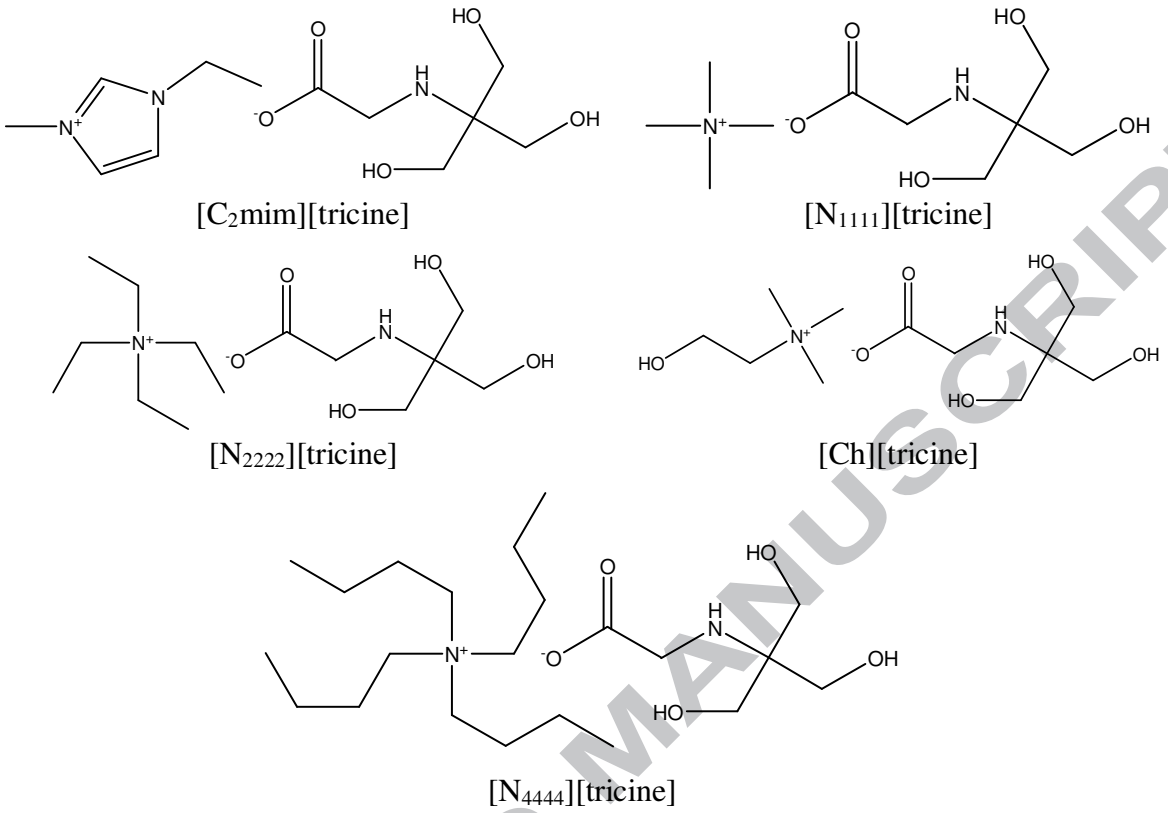

Fig. 2. Chemical structures of tricine and tricine-based Good's buffer ionic liquids.

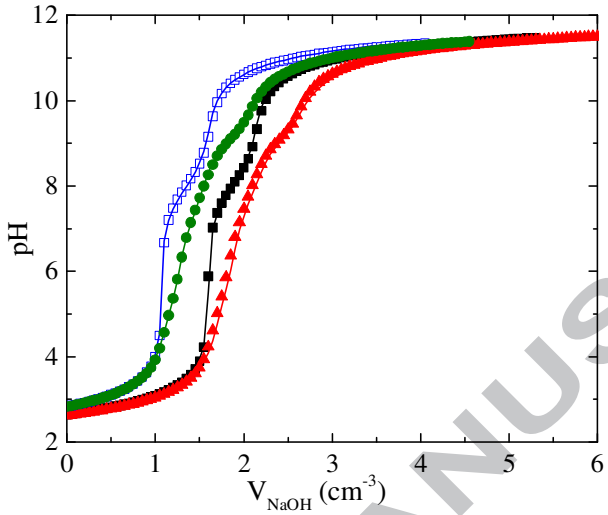

Fig. 3. pH titration curves of Eu(III) with tricine and [N_{4444}][tricine] at [T_L] = $1 \cdot 10^{-3}$ mol·dm^{-3} and [T_{Eu}] = $4 \cdot 10^{-4}$ mol·dm^{-3}, and at 298.2 K, I = 0.1 mol·dm^{-3} $NaNO_3$, and at 101.3 kPa. The symbols: (■) tricine; (▲) tricine + Eu(III); (□) [N_{4444}][tricine]; and (●)[N_{4444}][tricine] + Eu(III). The solid and dashed lines are the calculated pH from the refinement operations.

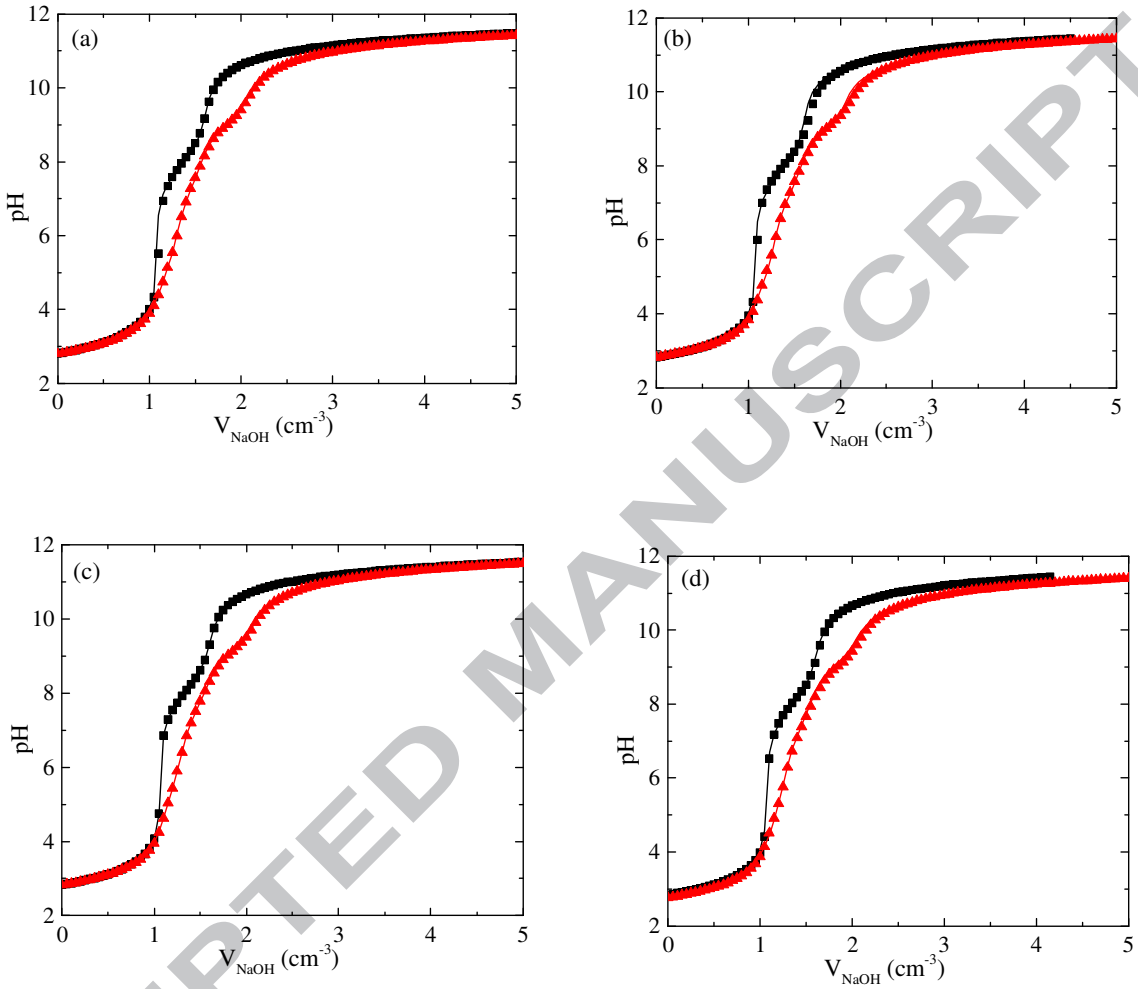

Fig. 4. pH titration curves of Eu(III) with (a) [C_4mim][tricine], (b) [Ch][tricine], (c) [N_{1111}][tricine], and (d) [N_{2222}][tricine] at $[T_L] = 1 \cdot 10^{-3}$ mol·dm^{-3} and $[T_{Eu}] = 4 \cdot 10^{-4}$ mol·dm^{-3}, and at 298.2 K, I = 0.1 mol·dm^{-3} $NaNO_3$, and at 101.3 kPa. The symbols: (■) tricine/IL and (▲) tricine/ILs + Eu(III). The solid and dashed lines are the calculated pH from the refinement operations.

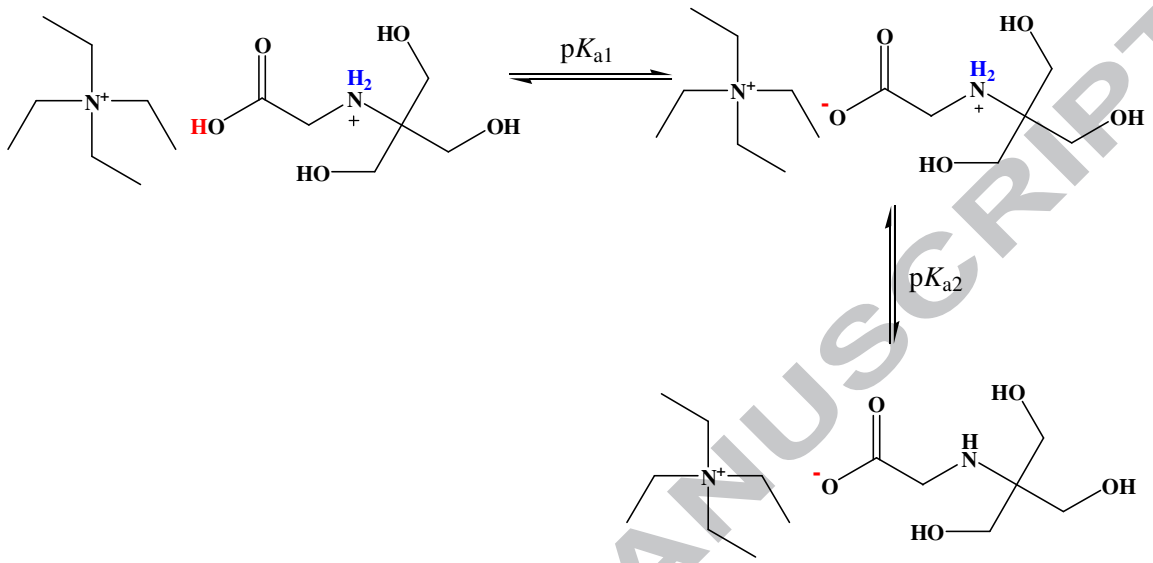

Fig. 5. The protonation equilibrium of [N_{2222}][tricine].

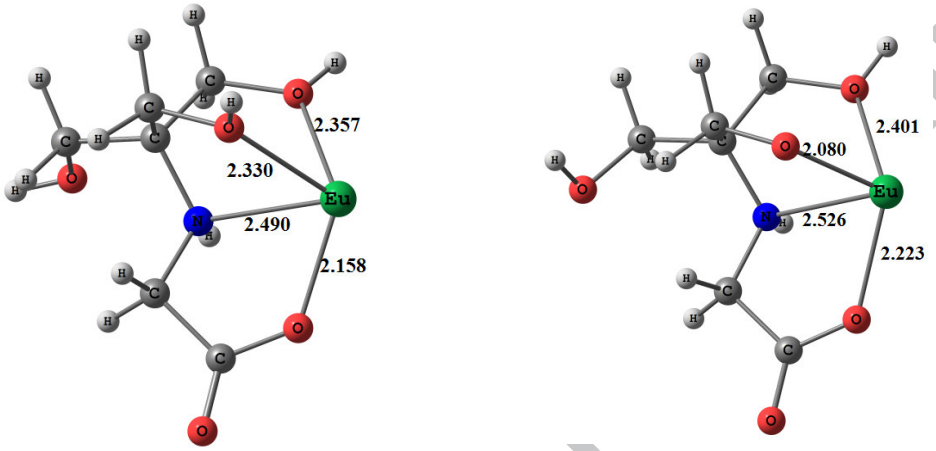

Fig. 6. The optimized structures of $Eu(tricine)^{2+}$ and $EuH_{-1}(tricine)^{+}$complexes with DFT/TZVP levels. The atom distances are in angstroms.

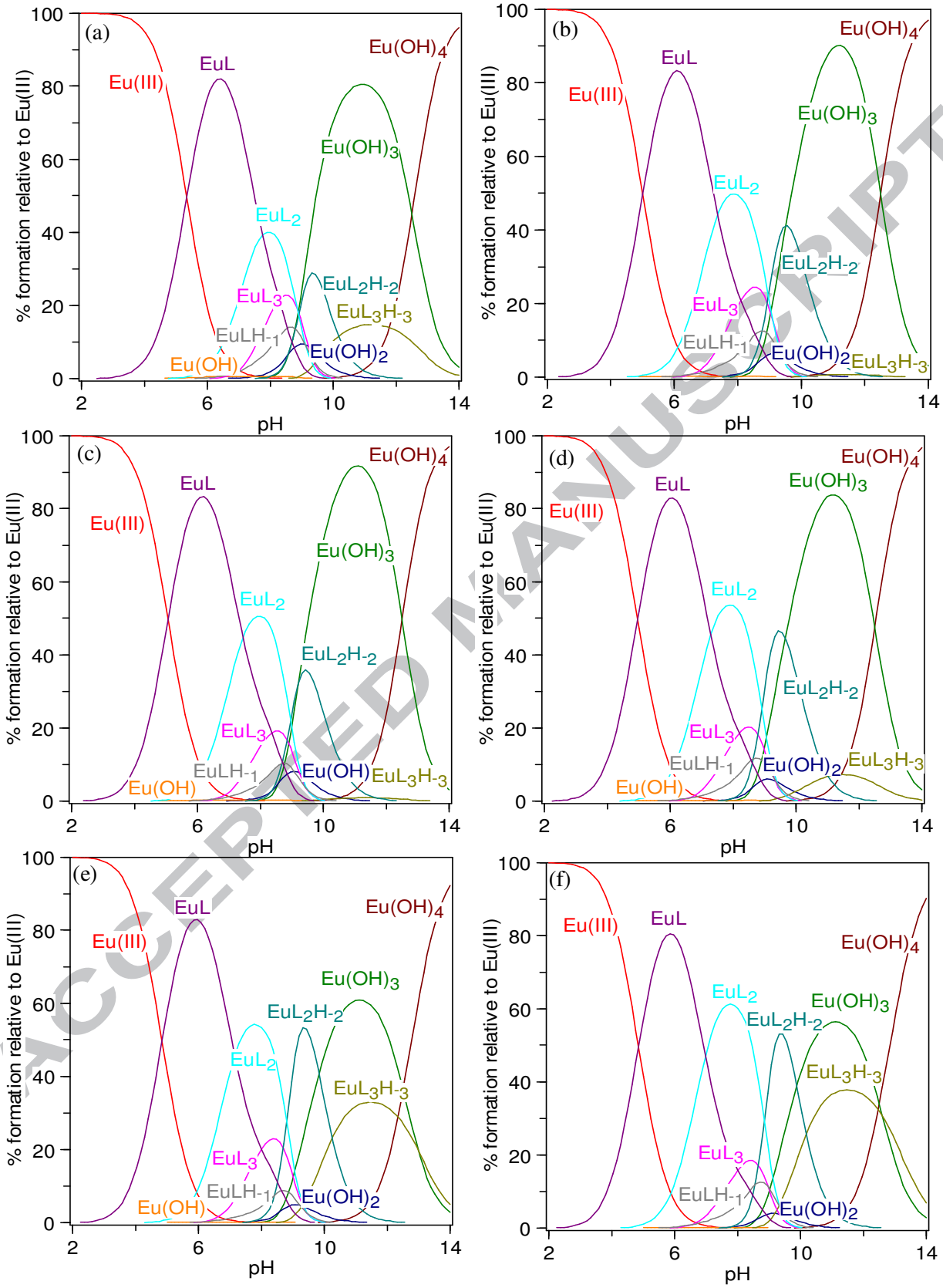

Fig. 7. Species-distribution diagrams of Eu(III) with (a) tricine, (b) $[N_{1111}]$[tricine], (c) $[N_{2222}]$[tricine], (d) $[N_{4444}]$[tricine], (e) [Ch][tricine], and (f) $[C_2mim]$[tricine]; [Eu] $=4.0\cdot10^{-4}$ mol·dm^{-3} and [L] $= 1.2\cdot10^{-3}$ mol·dm^{-3}; at 298.2 K, I = 0.1 mol·dm^{-3} $NaNO_3$, and at 101.3 kPa.

Highlights

- The protonation constants of tricine-based GB-ILs were determined.
- The stability constants of tricine-based GB-ILs with Eu(III) were determined.
- The studied GB-ILs have formed strong complexes with Eu(III) ion.
- The species distribution diagrams of these complexes were computed.
- The geometries of Eu-tricine complexes were characterized by DFT.

Coordination abilities of Good's buffer ionic liquids toward europium(III) ion in aqueous solution

*Mohamed Taha, Imran Khan, and João A. P. Coutinho**

CICECO-Aveiro Institute of Materials, Department of Chemistry, University of Aveiro, 3810-193 Aveiro, Portugal

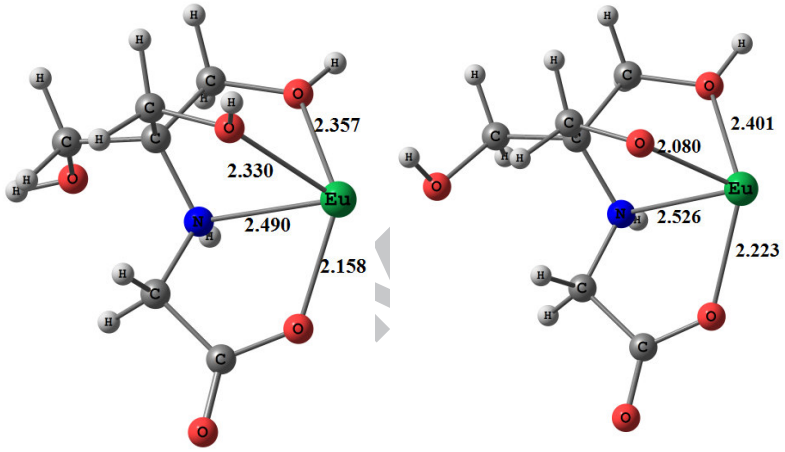

*Corresponding author. Tel.: +351 234 401 507; Fax: + 351 234 370 084

E-mail address: jcoutinho@ua.pt (J. A. P. Coutinho)